

COMPARISON OF LIGO/VIRGO UPPER LIMITS WITH PREDICTED COMPACT BINARY MERGER RATES

KRZYSZTOF BELCZYNSKI^{1,2}, MICHAŁ DOMINIŁ¹, SERENA REPETTO³, DANIEL E. HOLZ^{4,5}, CHRISTOPHER FRYER⁵

¹ Astronomical Observatory, University of Warsaw, Al. Ujazdowskie 4, 00-478 Warsaw, Poland

² Center for Gravitational Wave Astronomy, University of Texas at Brownsville, Brownsville, TX 78520, USA

³ Department of Astrophysics/IMAPP, Radboud University Nijmegen, PO Box 9010, 6500 GL Nijmegen, The Netherlands

⁴ Enrico Fermi Institute, Department of Physics, and Kavli Institute for Cosmological Physics, University of Chicago, Chicago, IL 60637

⁵ Theoretical Division, Los Alamos National Laboratory, Los Alamos, NM 87545

Draft version November 5, 2018

ABSTRACT

We compare the current LIGO/Virgo upper limits on double compact object volumetric merger rates with our theoretical predictions. Our optimistic models are a factor of ~ 3 below the existing upper limits for massive BH-BH systems with total mass $50\text{--}70 M_{\odot}$, suggesting that a small increase in observational sensitivity may bring the first detections. The LIGO/Virgo gravitational wave observatories are currently being upgraded to advanced design sensitivity. If a sizeable population of BH-BH binaries is detected, the maximum total binary mass of this population will discriminate between two general families of common envelope models. If no binaries are detected, the new upper limits will provide astrophysically useful information about the environment and physical processes (e.g., metallicity of host galaxies or BH natal kicks) crucial to the formation of binaries containing black holes. For NS-NS systems, our predicted rates are ~ 3 orders of magnitude below the current upper limits; even if advanced instruments reach their design sensitivities (factors of $10\times$ in distance, and $1,000\times$ in volumetric rate) the detection of NS-NS systems is not assured. However, we note that although our predicted NS-NS merger rates are consistent with estimates derived from Galactic NS-NS binaries and short GRBs, they are on the low side of these empirical estimates.

Subject headings: binaries: close — stars: evolution, neutron — gravitation

1. INTRODUCTION

Most massive stars are found in binary systems (Goodwin et al. 2007). During the evolution of these stars the binaries can experience component merger during common envelope (CE) phases (Webbink 1984) or disruption during supernova (SN) explosions (Tauris & Takens 1998) in which individual stars form neutron stars (NSs) or black holes (BHs). The massive binaries which survive these processes form double compact objects: NS-NS, BH-BH, or mixed BH-NS systems. These remnant systems are subsequently subject to angular momentum loss via the emission of gravitational waves (GWs) and their orbital separation decreases (Peters & Mathews 1963; Weisberg & Taylor 2005). Finally, the two compact objects collide and merge into a single compact object giving rise to a strong GW signal (Einstein 1918). The LIGO/Virgo network of ground-based interferometric observatories has been designed to search for these signals.¹

Initial LIGO/Virgo observations were concluded in 2012 without the detection of a GW signal. The instruments are currently being upgraded and the network will resume its operation in several years with advanced sensitivity. Various predictions for near-future detection chances were compiled and presented by Abadie et al. (2010).

One of the most promising sources for these advanced GW detectors is the inspiral and merger of binary NS systems. There are several known Galactic double neutron star binaries with merger times shorter than the Hubble time (e.g., Kim, Kalogera & Lorimer 2010). Double black hole binaries (BH-BH), on the other hand, remain unde-

tected. Recent theoretical predictions indicate that these systems may either dominate GW observations (e.g., Belczynski et al. 2010a) or be totally absent in local Universe (e.g., Mennekens & Vanbeveren 2013).

In this study we compare the rates from our evolutionary calculations of double compact object mergers (Dominik et al. 2012) with the existing LIGO/Virgo upper limits (Abadie et al. 2012; Aasi et al. 2013). We then make predictions for the science that will be probed with future upper limits and/or detections of double compact object mergers with advanced GW instruments.

2. CALCULATIONS

We have employed a set of publicly available evolutionary models (www.syntheticuniverse.org) that provide physical properties and Galactic merger rates (\mathcal{R}_{MW}) of NS-NS, BH-NS and BH-BH binaries. The calculations of the merger rates were obtained with the **StarTrack** population synthesis code (Belczynski et al. 2002, 2008), with the inclusion of crucial updates in the physical models (winds, SN, CE). We have chosen 12 physically realistic models, each testing one unknown in the evolutionary process leading to the formation of a NS-NS/BH-BH binary. For each model 2×10^6 primordial binaries were evolved, and we have converted the resulting Galactic merger rates to the volumetric local Universe merger rates using the formula:

$$\mathcal{R}_{\text{vol}} = 10^{-6} \rho_{\text{gal}} \left(f_{\text{Z}} \mathcal{R}_{\text{MW}}^{\text{Z}_{\odot}} + (1 - f_{\text{Z}}) \mathcal{R}_{\text{MW}}^{0.1\text{Z}_{\odot}} \right) \text{Mpc}^{-3} \text{yr}^{-1} \quad (1)$$

¹<http://www.ligo.caltech.edu/>; <https://www.cascina.virgo.infn.it/>

where $\mathcal{R}_{\text{MW}}^{Z_{\odot}}$ is the Galactic merger rate for models with solar-like metallicity ($Z = 0.02$) and $\mathcal{R}_{\text{MW}}^{0.1Z_{\odot}}$ is the Galactic merger rate for models with low metallicity ($Z = 0.002$). The Galactic merger rates ($\mathcal{R}_{\text{MW}}^{Z_{\odot}}, \mathcal{R}_{\text{MW}}^{0.1Z_{\odot}}$) are available from the aforementioned database and are expressed in Myr^{-1} . The fraction of the local stellar population with solar metallicity, as opposed to $0.1Z_{\odot}$, is given by f_Z . By altering this quantity we can construct local stellar populations with a range of metal content. We assume that a local density of Milky Way-like galaxies is $\rho_{\text{gal}} = 0.01 \text{ Mpc}^{-3}$.

The projected volumetric merger rates are listed in Table 1, sorted into bins of total binary mass (M_{tot}). The top row lists the LIGO upper limits on the rates from Abadie et al. (2012; see top panel of their Fig.4) for $M_{\text{tot}} < 25 M_{\odot}$, and from Aasi et al. (2013; see left panel of their Fig.5) for larger masses. These upper limits are for equal mass binaries; they are therefore the most stringent for a given total binary mass.

The standard model, denoted model S, employs the current best estimates for various physical parameters, including some that are not yet fully constrained but play an important role in the formation of double compact objects. For example: during CE evolution physical estimates of the donor binding energy are used (Xu & Li 2010), we adopt $M_{\text{NS,max}} = 2.5 M_{\odot}$ as the maximum NS mass (Lattimer & Prakash 2010), NS natal kicks are taken from observations as a single Maxwellian with $\sigma = 265 \text{ km s}^{-1}$ (Hobbs et al. 2005), BH kicks are smaller and obtained through a mass ejection mechanism (Fryer et al. 2012), the compact object mass spectrum is based on rapid supernova explosions (Belczynski et al. 2012), the stellar winds are revised for the effects of clumping (Belczynski et al. 2010b), and mass transfer episodes are non-conservative with 50% of the mass retained in the binaries (Meurs & van den Heuvel 1989).

In comparison to the standard model, we also run the following models. In models V5 and V6 we adopt $M_{\text{NS,max}} = 3.0, 2.0 M_{\odot}$, respectively. Natal kicks are decreased to $\sigma = 132.5 \text{ km s}^{-1}$ in V7 for NSs and BHs. High BH kicks ($\sigma = 265 \text{ km s}^{-1}$) and no BH kicks are adopted in V8 and V9, respectively. Delayed supernovae are employed in V10. The wind mass loss rate is decreased by factor 2 in V11. Conservative and fully non-conservative mass transfer is assumed in V12 and V13, respectively.

The investigation of $\sim 30,000$ Sloan Digital Sky Survey galaxies revealed that recent ($\sim 1 \text{ Gyr}$) star formation was bimodal with about half stars formed with high and half with low metallicity (Panter et al. 2008). Therefore, in all the aforementioned models we have evolved a 50%–50% combination of two stellar populations, one with high and one with low metallicity ($f_Z = 0.5$; see eq.1). To test the influence of metallicity on our predictions we also use a 90%–10% combination of metallicities, in which most stars are formed mostly at high metallicity ($f_Z = 0.9$). In model V16 this high metallicity combination is applied to the standard model while in model V17 it is applied to a high BH natal kick model (V8).

For each model we have tested whether the CE phase prevents the formation of NS-NS/BH-NS/BH-BH binaries (Belczynski et al. 2007). In particular, in the A models we allow for binary survival in the CE phase even if a donor

was a Hertzsprung gap (HG) star. It is not fully understood whether such stars have clear core-envelope structure and whether they will behave like MS stars (always resulting in a CE merger) or evolved giant stars (with potential CE survival). In the B models we assume that an HG donor always leads to a CE merger.

3. RESULTS

All of our models are fully described in Dominik et al. (2012). In what follows we list the most noteworthy trends, as well as compare directly with existing observational upper limits.

Our standard model calculation is presented in Figure 1. The dependence of the merger rate density on the total mass of the binary begins with a pronounced peak in the first mass bin ($M_{\text{tot}} = 2\text{--}5 M_{\odot}$) where all of the NS-NS systems and some of the BH-NS systems are found. The next mass bin ($M_{\text{tot}} = 5\text{--}8 M_{\odot}$) with relatively low merger rate densities contains mostly BH-NS systems. Then for higher mass bins merger rate density increases and the dependence is relatively flat, with a sharp rate density drop off at $M_{\text{tot}} \sim 70 M_{\odot}$ and $\sim 50 M_{\odot}$ for models A and B, respectively. Rate densities in model B are a factor of a few smaller than in model A. Model A rate densities are high, with $\mathcal{R}_{\text{vol}} \sim 10^{-8}\text{--}10^{-7} \text{ Mpc}^{-3} \text{ yr}^{-1}$. In particular, the predicted merger rate densities are only a factor of ~ 3 below the upper limits from LIGO/Virgo in the $M_{\text{tot}} = 54\text{--}73 M_{\odot}$ bin. Note that the predicted rates in the lowest mass bin are ~ 3 and ~ 2.5 orders of magnitude below the upper limits for models A and B, respectively.

A number of evolutionary models closely resemble the standard model: V5, V6, V7, V9, and V10 (see Table 1 for comparison). Several other models differ in various details from the standard model, but show an overall agreement in merger rate densities: V11, V12, and V13. Below we describe those models with significant differences from the standard model. These models represent a sequence of decreasing rate densities for massive binaries with $M_{\text{tot}} > 10 M_{\odot}$.

In model V14 we have altered the metallicity distribution of stellar populations in the local Universe to one with 90% of stars at high metallicity and 10% of stars at low metallicity. A majority of BH-BH binaries in our models form from low metallicity stars due to the lower wind mass loss rates and increased chance of CE survival (Belczynski et al. 2010a; Dominik et al. 2012). In model V14, therefore, we note an order of magnitude decrease (from the standard model, S) in the rate densities for massive mergers ($M_{\text{tot}} > 10 M_{\odot}$), resulting in rates of $\sim 10^{-8} \text{ Mpc}^{-3} \text{ yr}^{-1}$ (see Fig 2).

In model V8 we have increased the magnitude of BH natal kicks. Since this is one of the key factors in BH-BH formation, the results in a significant decrease in the rate density, to $\sim 10^{-9} - 10^{-8} \text{ Mpc}^{-3} \text{ yr}^{-1}$ (see Fig. 3). A significant increase in natal kicks (factor of ~ 4 ; see Discussion) leads to the disruption of progenitor binaries, thereby inhibiting BH-BH formation. In this model we do not use the kick mechanism based on asymmetric mass ejection during the supernova explosion that was adopted in our other models. During NS formation, exploding stars tend to be massive ($10\text{--}20 M_{\odot}$) in relation to the NS mass ($1.4 M_{\odot}$), and even a small asymmetry in the large ejected

mass imparts a significant momentum kick on a proto-NS. At BH formation the picture is qualitatively different, as the mass of a dying star is similar to the mass of the BH that is being formed. Most of the star mass is removed prior to the BH formation via intense stellar winds; e.g., Luminous Blue Variable phase and Wolf-Rayet phase (these winds are not expected for NS progenitors). Therefore very little mass ejection is predicted at BH formation, and natal kicks are expected to be insignificant. On the other hand, significant neutrino emission may be expected at formation of both neutron stars and black holes, possibly leading to high natal kicks in both cases.

Finally, in model V15 we have combined these two factors, high metallicity and high BH kicks, that limit BH-BH formation. As expected, this leads to a severe decrease in the rate density of massive mergers, to $\sim 10^{-10} - 10^{-9}$ $\text{Mpc}^{-3} \text{ yr}^{-1}$ (see Fig. 4). In particular, the rate densities are so low that even if the current LIGO/Virgo upper limits are increased by factor of 1,000 (corresponding to a factor of 10 in instrument distance sensitivity), no BH-BH mergers would be predicted to be detected.

4. DISCUSSION

4.1. NS-NS merger rates

Our predicted rates for NS-NS mergers are presented in Figures 1, 2, 3, 4 and the first mass bin of Table 1. These rates, although low, are consistent with available empirical estimates. Kim et al. (2010) have estimated NS-NS merger rate based on observations of three Galactic field NS-NS systems, B1913+16, B1534+12, and J0737-3039, and found a Galactic merger rate within the range 3–190 Myr^{-1} . O’Shaughnessy & Kim (2010) obtained a median value of 89 Myr^{-1} , with a spread above and below by a factor of ~ 3 when pulsar beaming constraints are taken into account. Kim, Perera & McLaughlin (2013) have re-examined the influence of double pulsar J0737-3039, obtaining a revised estimate of the Galactic merger rate of 7–49 Myr^{-1} , with median value 21 Myr^{-1} . None of these estimates include the large uncertainties in the pulsar luminosity function. If these uncertainties are included, it is expected that the rates could shift up or down by an order of magnitude (Richard O’Shaughnessy 2013, private communication). Applying this to the most recent estimate results in a broad range of allowed rates: 2.1–210 Myr^{-1} . For comparison, the Galactic merger rates in our standard evolutionary scenario are 23.5 and 7.6 Myr^{-1} for model A and B, respectively. Note that we list here only the rates for solar metallicity ($Z = 0.02$; i.e., Table 2 of Dominik et al. 2012) as these are relevant for Galactic field evolution where NS-NS binaries are found. Our NS-NS merger rates for sub-solar metallicity ($Z = 0.002$; i.e., Table 3 of Dominik et al. 2012) are factor of ~ 3 lower. The full spread of our rates for the solar metallicity models used in this study is 23.3–77.4 Myr^{-1} for the A models and 0.3–9.5 Myr^{-1} for the B models. Our predicted merger rates, while consistent with Galactic NS-NS observations, are on the lower end of empirical estimates.

There is a mounting evidence that short Gamma-ray bursts (GRBs) are connected with NS-NS and/or BH-NS mergers (e.g., Berger 2013), with some authors using short GRB rates to estimate NS-NS merger rates (e.g., Chen & Holz 2013). Fong et al. (2013) found short GRB rate den-

sities at the level 100–1,000 $\text{Gpc}^{-3} \text{ yr}^{-1}$, while Petrillo, Dietz, & Cavagila (2013) estimated the rate density to be 500–1,500 $\text{Mpc}^{-3} \text{ yr}^{-1}$. These results suffer short GRB beaming and luminosity uncertainties. The beaming has been firmly established for ~ 3 short GRBs (with $\theta_j \lesssim 10$ deg), while redshifts and thus luminosities are only known for the ~ 20 closest events. It is possible that the average beaming angle is larger than currently estimated, and that the rates densities are correspondingly lower, possibly by an order of magnitude (Edo Berger 2013, private communication). The lower limit on the short GRB rate density would then decrease to 10–50 $\text{Gpc}^{-3} \text{ yr}^{-1}$. Before comparing with our NS-NS merger rate density it is worth noting that even if NS-NS stars are in fact short GRB progenitors, they may be responsible for only a fraction of short GRBs as other progenitors cannot be excluded at the moment (e.g., Nakar 2010). On the other hand only some fraction of NS-NS mergers may produce short GRBs. The NS-NS merger rate densities that we have adopted from Dominik et al. (2012) are at the level of 50 and 150 $\text{Gpc}^{-3} \text{ yr}^{-1}$ for our standard model calculation for submodels B and A, respectively. We have employed a 50%–50% combination of high and low metallicity stellar populations ($f_Z = 0.5$) since short GRBs are found in host galaxies with a range of metallicities. Note that the NS-NS rate density can only be approximately read off Table 1, as the first mass bin contains both NS-NS and BH-NS mergers. However, NS-NS mergers dominate in this bin, so the first mass bin is a good approximation for the overall NS-NS merger rate density. The clear cut division between NS-NS and BH-NS merger rates is given in Dominik et al. (2012). Again, we note that our rate predictions are consistent with short GRB observations, although they are found somewhat on the low side of empirical estimates.

4.2. BH natal kicks

The current models behind natal kicks involve asymmetric mass ejection in supernova explosions leading to high NS kicks and small BH kicks (e.g., Herant, Benz, Colgate 1992; Blondin, Mezzacappa, DeMarino 2003). However, at the moment the possibility that BHs receive high natal kicks through some other mechanism (e.g., asymmetric neutrino emission; Lai 2001 and references within) cannot be excluded on theoretical grounds.

In our standard model we employ natal kicks that are associated with asymmetric mass ejection, while in model V8 we assume high BH natal kicks (e.g., from asymmetric neutrino emission). Comparison of rate densities for both models clearly demonstrates a significant decrease of BH-BH systems due to high BH kicks. We conclude that natal BH kicks are one of the most important factors in determining the number of BH-BH systems.

Thus far the only empirical approach to get insights into the natal kicks black holes receive at birth, is achieved by following both the Galactic dynamics and the binary evolution of black-hole X-ray binaries (BH-XRBs), which are semi-detached binaries where a companion star, either of low-mass or high-mass, is transferring material to a black hole. The natal kick at birth changes the Galactic position and the space velocity of the binary, as well as the binary orbital properties. Tracing the binary evolution and the trajectory of the binary backwards in time, it is then possible to place constraints on the natal kick the black hole

receives. This approach has been applied in the past to a handful of sources, and seems to point towards a dichotomous scenario for the black-hole natal kicks. Small natal kicks, of the order of few tens of km s^{-1} are found for GRO J1655-40 (Willems et al. 2005), and for Cygnus X-1 (Wong et al. 2012); whereas evidence for an intermediate to high natal-kick is found for XTE J1118+480, a BH-XRB which requires a natal kick in the range $80 - 310 \text{ km s}^{-1}$ (Fragos et al. 2009). Repetto, Davies & Sigurdsson (2012) performed an analysis of positions and velocities of most known Galactic BH-XRBs. They constrain the natal kick by making sure that the binary after-kick orbital configuration is consistent with the observed one, and at the same time that the natal kick is high enough to place the binary in the current height from the Galactic plane, assuming it was born on the plane. The natal kick they obtain is an absolute lower-limit, the space velocity in the post-supernova configuration being in the optimal direction, i.e. perpendicular to the Galactic plane. They found that 9 BHs do not require any or only a small kick ($\sim 0-40 \text{ km s}^{-1}$; XTE J1550-564, GRO J1655-40, GRS 1915+105, GS 2023+338, GRO J0422+32, A0620-003, GRS 1009-45, 1124-683, GS 2000+251), 2 BHs require intermediate kicks ($\sim 80 \text{ km s}^{-1}$; 4U 1543-47, XTE J1118+480) and the other two require high kicks ($190, 450 \text{ km s}^{-1}$ for 1819.3-2525 and 1705-250, respectively) comparable to pulsar kicks. Repetto & Nelemans (in preparation) combines the study of BH-XRB positions and velocities with detailed binary evolution calculation. They trace the binary evolution of the systems backwards until the post-supernova configuration. Their results are consistent with the ones in Repetto et al. (2012), and show evidence for black hole receiving intermediate or high kicks in at least some of the sources. In Table 2 we show the collected data on BH natal kick estimates along with BH mass estimates for 14 Galactic BH-XRBs. The natal kick estimates are lower limits on the natal kick, the space velocity being in the optimal direction.

In Figure 5 we show these observational estimates along with our standard and high BH kick models. Both the BH kicks and the mass estimates suffer large uncertainties which we choose not to plot to allow a clearer comparison of trends in the observations and theoretical predictions. For the theoretical models we show the average values of the kick. High BH kicks are modeled as a (mass independent) 1D Maxwellian distribution of kicks with $\sigma = 265 \text{ km s}^{-1}$, with an average at 420 km s^{-1} . For our standard model the kick is drawn from a Maxwellian with $\sigma = 265 \text{ km s}^{-1}$, with the value decreased inversely proportional to the amount of fall back mass at BH formation in the core collapse/supernova explosion. The amount of fall back is estimated from rapid supernova models that reproduce the observed mass gap between NSs and BHs in Galactic X-ray binaries (Belczynski et al. 2012). The non-monotonic dependence of fall back on BH (and progenitor) mass is discussed and explained in Appendix. As clearly seen from Figure 5, while neither of the models can explain all the empirical estimates, the standard model with low BH kicks associated with asymmetric mass ejection appears to be a better match to the available observations.

5. CONCLUSIONS

Our results show that a small improvement in LIGO/Virgo’s current sensitivity to double compact object mergers, by a factor of $\sqrt[3]{3}$ in distance (factor of 3 in volume), will either bring the first detections of massive BH-BH binaries ($M_{\text{tot}} > 50 M_{\odot}$) or through non-detection exclude entire families of evolutionary models (see the proximity of Model A to the LIGO/Virgo upper limits in Figure 1).

If discoveries of massive BH-BH binaries are made, even at low rates, it will indicate that stars just beyond the main sequence (i.e., on the Hertzsprung gap) survive common envelope and form close double compact objects (see Figures 1, 2, 3, and differences between models A and B).

If upper limits are improved by a factor of 100 and we remain without the detection of BH-BH binaries, it will indicate that other factors than common envelope are responsible for eliminating the BH-BH formation channels. Our analysis indicates that high black hole natal kicks and high metallicity stellar environments are two crucial factors that significantly reduce the BH-BH merger rates (see Figures 2, 3 and the associated merger rate reductions). These two factors show a degeneracy when it comes to the rate of BH-BH mergers, so additional constraints are required to distinguish their relative importance.

If upper limits are improved by factor of 1,000 and no BH-BH discoveries are made, then the above degeneracy is lifted and we can conclude that BHs receive high natal kicks *and* that the stellar populations within reach of LIGO are typically of high (solar-like) metallicity (see Figure 4, where the BH-BH rates fall below the enhanced upper limits). This is demonstrated by our V15 model in which we have increased the magnitude of BH natal kicks and the high metallicity content of the local Universe to the largest values with reasonable limits: it is difficult to imagine BHs receiving higher kicks than NSs (see Figure 5), and less than 10% of stars in the local Universe having sub-solar metallicity (e.g., Panter et al. 2008).

The above conclusions apply only within the framework of our evolutionary model. Our model successfully recovers the observed BH mass spectrum both in the Galaxy and in other environments (Belczynski et al. 2010b). It also provides a physical explanation for the existence of the mass gap between neutron stars and black holes, failing to produce compact objects in the mass range $2-5 M_{\odot}$ (Belczynski et al. 2012). However, our model is unable to reproduce the companion mass distribution observed in Galactic BH transients. The observed distribution peaks at $\sim 0.6 M_{\odot}$ while most of our predicted distributions peak at $\sim 1 M_{\odot}$. This discrepancy may arise from our poor understanding of magnetic braking in these low mass companions along with uncertainties in low mass stellar models. It is also possible that the discrepancy arises from observational biases (Wiktorowicz, Belczynski, & Maccarone 2013). These factors should not play a significant role in the modeling of massive stars and the formation of NS-NS, BH-NS, or BH-BH binaries.

A different reduction factor in BH-BH formation was proposed by Mennekens & Vanbeveren (2013). These authors claim that strong Luminous Blue Variable (LBV) winds may inhibit formation of close BH-BH binaries. They argue that the action of these very intense winds from BH progenitors leads to an increase in orbital separa-

ration such that BH-BH binaries with merger times below a Hubble time no longer form. This finding is hard to reconcile with observations, as a number of Galactic and extra-galactic binaries with black holes on close orbits are known (e.g., extra-galactic IC10 X-1 with $P_{\text{orbital}} = 33$ h or Galactic GRO J0422+32 with $P_{\text{orbital}} = 5.1$ h both hosting massive $\gtrsim 10 M_{\odot}$ BHs).

If NS-NS mergers are found before the advanced instruments reach their design sensitivity (a improvement by a factor of $\sim 1,000$ in volume) it will indicate that our predicted NS-NS merger rates densities are too low. The astrophysical implications of such a potential finding are now under study (Dominik et al., in preparation). Alternatively, it is worth noting that even with an increase in the existing upper limits by factor of $\sim 1,000$ some of our model predictions, as well as low values of rates derived from observations of Galactic NS-NS binaries and cosmic short GRBs, allow for the possibility of non-detection of NS-NS mergers (see Figure 4; some of our models, as well as empirical estimates, allow for lower merger rate densities than those shown).

In conclusion, there exist a wide range of possibilities for the rates of compact binary mergers in advanced detectors

like LIGO and Virgo. The first detections may be made with small improvements over the instruments sensitivity. Alternatively, even at full advanced design sensitivity there may be no detections of double compact object mergers. Regardless of whether there are detections or more stringent upper limits on the rates, LIGO/Virgo will address a number of important science problems in our understanding of compact binary formation and evolution.

KB and MD acknowledge support from NCN grant SONATA BIS and FNP professorial subsidy MASTER2013 and NASA Grant NNX09AV06A to the UTB. MD acknowledges support from NCN grant 2011/01/N/ST9/00383. DEH acknowledges support from National Science Foundation CAREER grant PHY-1151836. The work of C.F. was done under the auspices of the National Nuclear Security Administration of the U.S. Department of Energy, and supported by its contract DEAC52-06NA25396 at Los Alamos National Laboratory. We would like to thank T.Bulik, I.Mandel, T.Piran, P.Brady, A.Buonanno for critical and constructive comments on the results presented in this study.

REFERENCES

- Aasi, J., et al. 2013, *Phys. Rev. D.*, 87, 022002
 Abadie, J., et al. 2010, *CAQG*, 27, 173001
 Abadie, J., et al. 2012, *Phys. Rev. D*, 85, 082002
 Belczynski, K., Kalogera, V., Bulik, T. 2002, *ApJ*, 572, 407
 Belczynski, K., et al. 2007, *ApJ*, 662, 504
 Belczynski, K., et al. 2008, *ApJS*, 174, 223
 Belczynski, K., et al. 2010a, *ApJ*, 715, L138
 Belczynski, K., et al. 2010b, *ApJ*, 714, 1217
 Belczynski, K., Wiktorowicz, G., Fryer, C., Holz, D., & Kalogera, V. 2012, *ApJ*, 757, 91
 Berger, E. 2013, *ARAA*, 51, accepted (arXiv:1311.2603)
 Blondin, J., Mezzacappa, A., DeMarino, C. 2003, *ApJ*, 584, 971
 Cantrell, J., et al. 2010, *ApJ*, 710, 1127
 Chen, H.-Y., & Holz, D.E. 2013, *PRL*, 111, 181101
 Dominik, M., et al. 2012, *ApJ*, submitted (arXiv:1202.4901)
 Einstein, A. 1918, *Über Gravitationswellen*, *Sitzungsberichte der physikalisch-mathematischen Klasse*, 1, 154
 Fong, W., et al. 2012, *ApJ*, 756, 189
 Fragos, T., Willems, B., Kalogera, V., Ivanova, N., Rockefeller, G., Fryer, C.L., & Young, P.A. 2009, *ApJ*, 697, 1057
 Fryer, C., et al. 2012, *ApJ*, 749, 91
 Gelino, D., Harrison, T., & McNamara, B. 2001, *ApJ*, 122, 971
 Goodwin S. P., Kroupa P., Goodman A., Burkert A. 2007, in Reipurth B., Jewitt D., Keil K., eds, *Protostars and Planets V: The Fragmentation of Cores and the Initial Binary Population*, p.133
 Greene, J., Bailyn, C., & Orosz, J. 2001, *ApJ*, 554, 1290
 Harlaftis, E., et al. 1997, *AJ*, 114, 1170
 Herant, M., Benz, W., & Colgate, S. 1992, *ApJ*, 395, 642
 Hobbs, G., Lorimer, D. R., Lyne, A. G., & Kramer, M. 2005, *MNRAS*, 360, 974
 Ioannou, Z., Robinson, E., Welsh, F., & Haswell, C. 2004, *AJ*, 127, 481
 Khargharia, J., Froning, C., Robinson, E., & Gelino, D. 2013, *AJ*, 145, 21
 Kim, C., Kalogera, V., & Lorimer, D. 2010, *New Astr. Rev.*, 54, 148
 Kim, C., Perera, B., & McLaughlin, M. 2013, *MNRAS*, submitted (arXiv:1308.4676)
 Kuulkers, E., et al., *A&A*, submitted (arXiv:1204.5840)
 Lai, D. 2001, in *Physics of Neutron Star Interiors*, ed. by D. Blaschke, N.K. Glendenning and A. Sedrakian, *Lecture Notes in Physics*, vol. 578, p.424
 Lattimer, J., & Prakash, M. 2010, To appear in *Gerry Brown's Festschrift*; Editor: Sabine Lee (World Scientific) (arXiv:1012.3208)
 Li, Z., Qu, J., Song, L., Ding, G., & Zhang, C. 2013, *MNRAS*, 428, 1704
 Macias, P., et al. 2011, in *AAS 217*, Vol. 43, 143.04
 Martin, R., Reis, R., & Pringle, J. 2008, *MNRAS*, 391, L15
 Mennekens, N., & Vanbeveren, D. 2013, *A&A*, submitted (arXiv:1307.0959)
 Meurs, E. & van den Heuvel, E. 1989, *A&A*, 226, 88
 Mirabel, F., & Rodrigues, I. 2003, *Science*, 300, 1119
 Nakar, E. 2010, proceedings of the *The Shocking Universe meeting* (arXiv:1009.4648)
 Orosz, J., Jain, R., Bailyn, C., McClintock, J., & Remillard, R. 1998, *ApJ*, 499, 375
 Orosz, J., McClintock, J., Aufdenberg, J., Remillard, R., Reid, M., Narayan, R., & Gou, L. 2011, *ApJ*, 742:84.
 O'Shaughnessy, R., Kim, C. 2010, *ApJ*, 715, 230
 Panter, B., Jimenez, R., Heavens, A., & Charlot, S. 2008, *MNRAS*, 391, 1117
 Peters, P., & Mathews, J. 1963, *Phys. Rev.*, 131, 435
 Petrillo, C., Dietz, A., & Cavagila, M. 2013, *ApJ*, 767, 140
 Reid, M., et al. 2011, *ApJ*, 742, 83
 Repetto, S., Davies, M., & Sigurdsson, S. 2012, *MNRAS*, 425, 2799
 Repetto, S., Nelemans, G., in prep.
 Reynolds, M., Callanan, P., & Filippenko, A. 2007, *MNRAS*, 374, 657
 Shahbaz, T., Ringwald, F., Bunn, J., Naylor, T., Charles, P., & Casares, J. 1994, *MNRAS*, 271, L10
 Steeghs, D., et al. 2013, *ApJ*, 768, 185
 Tauris, T., & Takens, R. 1998, *A&A*, 330, 1047
 Webbink, R. 1984, *ApJ*, 277, 355
 Weisberg, J., & Taylor, J. 2005, in *Binary Radio Pulsars*, ASP Conference Series, Vol. 328, Edited by F. A. Rasio and I. H. Stairs. San Francisco: Astronomical Society of the Pacific, p.25
 Wiktorowicz, G., Belczynski, K., Maccarone, T. 2013, *ApJ*, submitted (arXiv:1312.5924)
 Willems, B., Henninger, M., Levin, T., Ivanova, N., Kalogera, V., McGhee, K., Timmes, F.X., & Fryer, C.L. 2005, *ApJ*, 625, 324
 Wong, T.-W., Valsecchi, F., Fragos, T., & Kalogera, V. 2012, *ApJ*, 747, 111
 Xu, X., & Li, X. 2010, *ApJ*, 716, 114

TABLE 1
DOUBLE COMPACT OBJECT MERGER RATE DENSITY [MPC⁻³ YR⁻¹] ^a

Model	Total	$M_{\text{tot}} / M_{\odot} =$										
		2-5 ^b	5-8	8-11	11-14	14-17	17-20	20-25	25-37	37-54	54-73	73-91 ^c
LIGO ^d	—	7.5e-5	2.5e-5	1.0e-5	7.5e-6	5.0e-6	3.8e-6	3.2e-6	8.7e-7	3.3e-7	1.7e-7	0.9e-7
S A	5.9e-7	1.6e-7	6.1e-10	1.7e-8	3.3e-8	1.2e-7	3.1e-8	5.1e-8	8.3e-8	4.7e-8	5.4e-8	1.4e-10
B	1.4e-7	5.0e-8	1.6e-10	5.4e-9	9.3e-9	2.8e-8	5.4e-9	1.6e-8	2.5e-8	1.3e-9	0	0
V5 A	5.9e-7	1.6e-7	7.1e-10	1.6e-8	3.3e-8	1.1e-7	3.0e-8	5.1e-8	8.5e-8	4.7e-8	5.5e-8	1.2e-10
B	1.4e-7	5.2e-8	1.9e-10	5.2e-9	9.2e-9	2.9e-8	5.1e-9	1.6e-8	2.5e-8	1.5e-9	0	0
V6 A	6.0e-7	1.6e-7	6.5e-10	1.7e-8	3.4e-8	1.2e-7	3.2e-8	5.5e-8	8.3e-8	4.5e-8	5.5e-8	1.9e-10
B	1.4e-7	5.2e-8	1.7e-10	5.0e-9	8.5e-9	2.8e-8	5.2e-9	1.8e-8	2.4e-8	1.4e-9	0	0
V7 A	7.1e-7	2.0e-7	1.5e-9	2.6e-8	5.2e-8	1.4e-7	4.6e-8	6.2e-8	8.4e-8	4.6e-8	5.3e-8	9.6e-11
B	1.7e-7	5.8e-8	7.1e-10	1.1e-8	1.2e-8	3.0e-8	9.0e-9	2.0e-8	2.5e-8	1.4e-9	0	0
V8 A	1.8e-7	1.6e-7	3.1e-10	2.3e-9	3.9e-9	7.6e-9	3.1e-9	3.1e-9	2.9e-9	4.8e-10	7.7e-10	1.0e-10
B	5.7e-8	5.2e-8	0	6.9e-10	1.4e-9	2.0e-9	2.1e-10	2.7e-10	3.4e-10	7.4e-11	0	0
V9 A	7.4e-7	1.6e-7	1.6e-9	2.3e-8	7.7e-8	1.6e-7	5.4e-8	6.8e-8	8.6e-8	4.7e-8	5.4e-8	1.2e-10
B	1.9e-7	5.2e-8	1.1e-9	1.1e-8	1.9e-8	3.9e-8	1.6e-8	2.5e-8	2.6e-8	1.4e-9	0	0
V10A	5.0e-7	1.7e-7	2.5e-9	1.1e-8	2.1e-8	2.3e-8	2.9e-8	5.2e-8	8.6e-8	4.8e-8	5.3e-8	1.5e-10
B	1.3e-7	5.7e-8	1.3e-9	4.0e-9	7.6e-9	4.7e-9	7.7e-9	1.6e-8	2.6e-8	1.3e-9	0	0
V11A	7.3e-7	1.6e-7	6.6e-10	1.2e-8	3.3e-8	1.1e-7	3.3e-8	7.5e-8	2.0e-7	5.0e-8	2.7e-8	3.6e-8
B	1.6e-7	4.4e-8	0	2.3e-9	9.6e-9	3.0e-8	5.6e-9	1.8e-8	4.7e-8	4.2e-9	0	0
V12A	8.8e-7	4.7e-7	1.4e-10	9.3e-9	2.2e-8	6.7e-8	4.5e-8	6.7e-8	8.7e-8	5.0e-8	6.3e-8	2.0e-10
B	7.8e-8	2.3e-8	1.2e-10	6.5e-9	9.3e-9	1.4e-8	3.4e-9	7.7e-9	1.4e-8	8.8e-10	0	0
V13A	6.0e-7	1.6e-7	4.7e-9	1.6e-7	4.9e-8	7.8e-8	3.5e-8	5.4e-8	4.4e-8	1.0e-8	6.3e-9	0
B	3.6e-7	3.8e-8	2.1e-9	1.2e-7	2.8e-8	4.4e-8	2.4e-8	4.9e-8	4.3e-8	5.6e-9	0	0
V16A	3.9e-7	2.2e-7	2.0e-10	1.6e-8	1.5e-8	8.1e-8	6.6e-9	1.0e-8	1.6e-8	9.3e-9	1.1e-8	2.7e-11
B	1.1e-7	7.2e-8	1.1e-10	2.6e-9	3.2e-9	1.9e-8	1.2e-9	3.2e-9	5.0e-9	2.5e-10	0	0
V17A	2.3e-7	2.2e-7	6.5e-11	6.4e-10	8.9e-10	1.8e-9	6.6e-10	6.2e-10	5.9e-10	1.0e-10	1.5e-10	1.7e-11
B	7.5e-8	7.4e-8	0	1.7e-10	3.2e-10	4.4e-10	4.2e-11	5.2e-11	6.9e-11	1.2e-11	0	0

^a Rate densities are given under the assumption that the CE phase initiated by Hertzsprung gap donors may lead to the formation of a double compact object binary (A) or always halts binary evolution (B).

^b Our binning corresponds to the LIGO/Virgo low and high mass search bins.

^c We do not show results for the last mass bin $M_{\text{tot}} = 91\text{--}109 M_{\odot}$, as the rates are zero in this bin for all models but V11A, the latter with a rate of $4.9 \times 10^{-11} \text{ Mpc}^{-3} \text{ yr}^{-1}$. For comparison, the LIGO/Virgo upper limit for this bin is $0.7 \times 10^{-7} \text{ Mpc}^{-3} \text{ yr}^{-1}$.

^d Available initial LIGO/Virgo upper limits for equal mass mergers are listed.

TABLE 2
BLACK HOLE MASS AND NATAL KICK ^a

No	Name	Mass [M_{\odot}]	Natal Kick [km s^{-1}]
1)	4U 1543-47	5.1 (1)	80 (2)
2)	GRO J1655-40	6.3 (3)	30 (4)
3)	H 1705-250 (Nova Oph 77)	6.4 (5)	450-460 (2,6) ^b
4)	GS 2000+251	6.55 (7)	0-20 (2,6)
5)	A0620-00 (V616 Mon)	6.6 (8)	0-10 (2,6)
6)	GRS 1124-68 (Nova Mus 91)	6.95 (9)	40-60 (2,6) ^c
7)	XTE J1118+480	7.6 (10)	70-80 (2,11)
8)	GRS 1009-45	8.5 (12)	15-50 (2,6)
9)	GRS 1915+105	10.1 (13)	0 (2)
10)	XTE J1819-254 (V4641 Sgr)	10.2 (14)	190 (2) ^d
11)	GRO J0422+32	10.4 (15)	10-30 (2,6)
12)	XTE J1550-564	10.5 (16)	10 (2)
13)	GS 2023+338 (V404 Cyg)	12 (17)	0 (2)
14)	Cyg X-1	14.8 (18)	0-55 (19,20)

^a References for the mass and natal kick estimates are given in parentheses: (1) Orosz et al. (1998), (2) Repetto et al. 2012, (3) Greene et al. (2001), (4) Willems et al. (2005), (5) Harlaftis et al. (1997), (6) Repetto & Nelemans (in prep), (7) Ioannou et al. (2004), (8) Cantrell et al. (2010), (9) Gelino et al. (2001), (10) Khargharia et al. (2013), (11) Fragos et al. (2009), (12) Macias et al. (2011), (13) Steeghs et al. (2013), (14) Martin et al. (2008), (15) Reynolds et al. (2007), (16) Li et al. (2013), (17) Shahbaz et al. (1994), (18) Orosz et al. (2011), (19) Mirabel & Rodrigues (2003), (20) Wong et al. (2012).

^bMarked as 1705-250 in Repetto et al. (2012).

^cMarked as 1124-683 in Repetto et al. (2012).

^dMarked as 1819.3-2525 in Repetto et al. (2012).

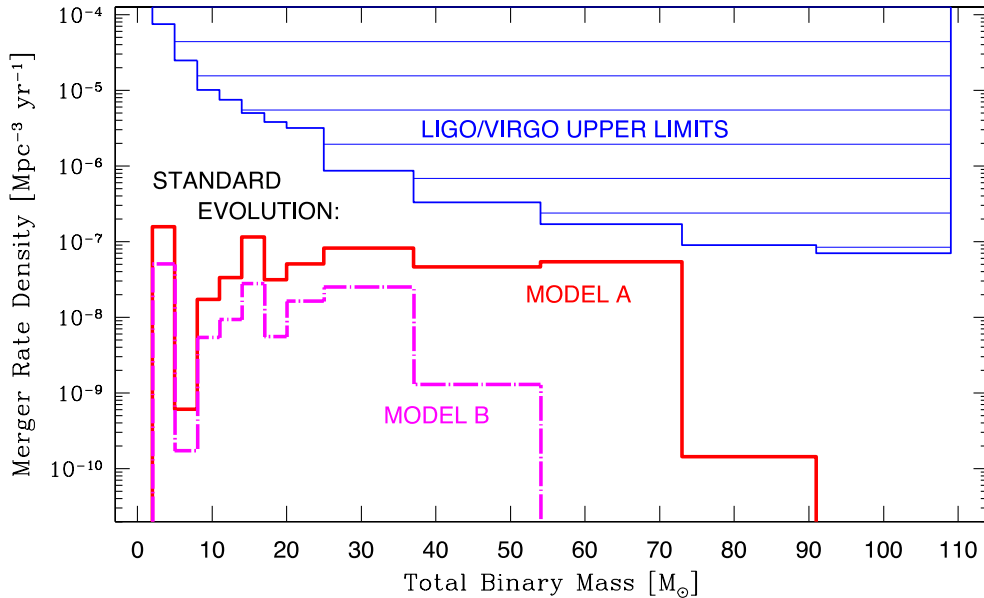


Fig. 1.— Rate density of double compact object mergers for our standard evolutionary calculation. The solid line represents our population synthesis model in which we allow for CE survival with HG donors (model A). The dashed-dotted line shows a model in which CE events with HG donors are not allowed (model B). Most of our evolutionary variations (e.g., V5, V6, V7, V9, V10) are indistinguishable from the standard prediction. Note that model B is characterized by lower rate densities (down by a factor of a few in each mass bin) and a significant rate density drop off occurs at much smaller total binary mass ($M_{\text{tot}} = 35 M_{\odot}$) than for model A ($M_{\text{tot}} = 70 M_{\odot}$). The top shaded area shows the upper limits from initial LIGO/Virgo.

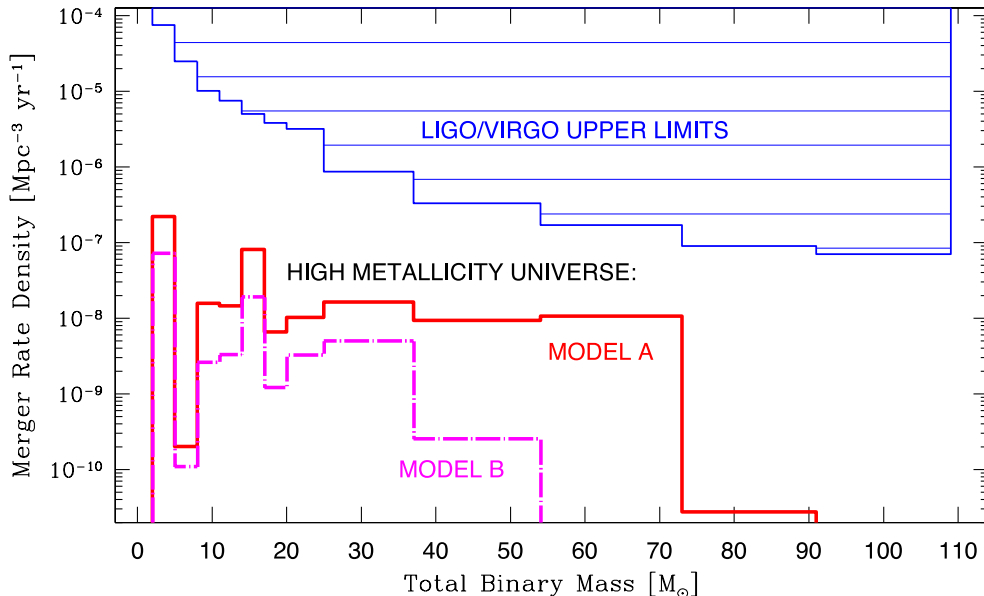


Fig. 2.— Rate density of double compact object mergers for our standard evolution with one change—we consider a toy universe with a high content of high metallicity stars: 90% of stars with $Z = Z_{\odot}$ and 10% with $Z = 0.1 Z_{\odot}$ (V14). For comparison, the rest of our models were obtained with a low content of high metallicity stars: 50% of stars with $Z = Z_{\odot}$ and 50% with $Z = 0.1 Z_{\odot}$. Note the moderate decrease in rate density of high mass mergers in both the A and B models as compared with the low metallicity standard model (Fig. 1).

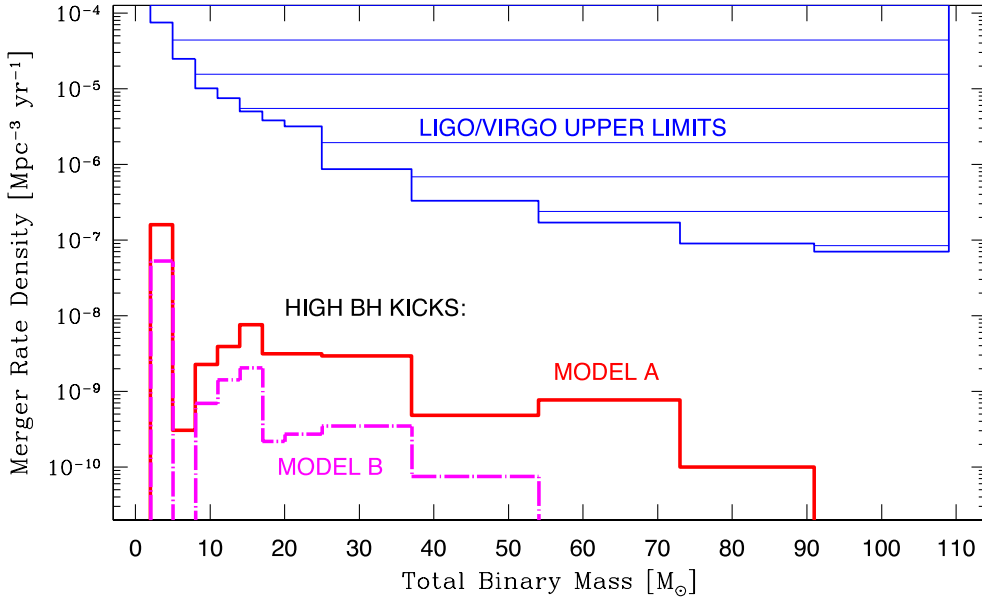


Fig. 3.— Rate density of double compact object mergers for the high BH kick model (V8). Note the significant decrease in rate density for both the A and B models as compared with the standard evolutionary scenario (low or no BH kicks). However, the distinctive behavior of models A and B (i.e. differing maximum mass of merging binary) is the same as in the standard model case.

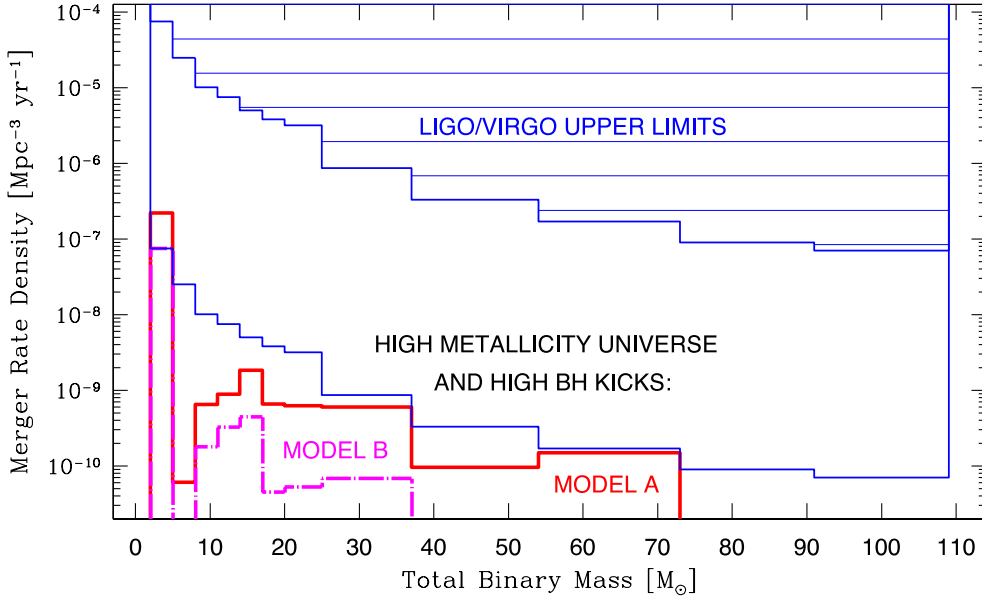


Fig. 4.— Rate density of double compact object mergers for the combined high metallicity and high BH kick model (V15). We also show improved (by a factor of 1,000) upper limits expected from advanced sensitivity instruments. Note that in this model all BH-BH binaries are just below the improved upper limits; it would not predict any detections.

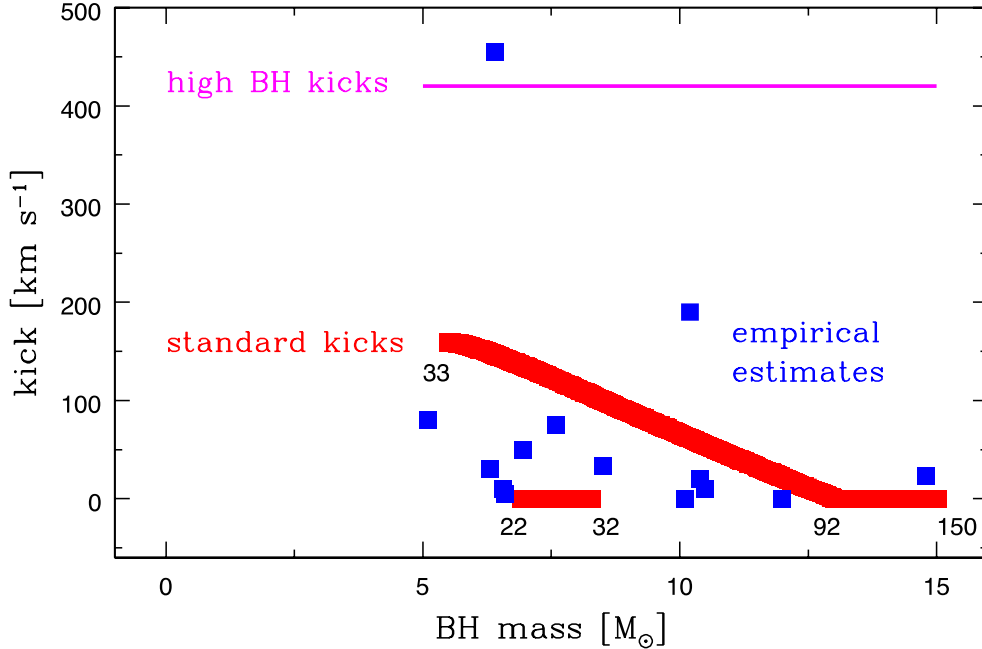


Fig. 5.— Average black hole natal kick adopted in our calculations. In our standard model the kicks decrease with increasing mass of the black hole (red). Zero kicks (direct collapse) are found for the highest mass black holes as well as for medium mass black holes, the latter reflecting the physics of our core collapse/supernova model (rapid explosion of Fryer et al. 2012). The kicks are drawn from a Maxwellian distribution with a kick magnitude decreasing with increasing fall back mass estimated at each black hole’s formation. In our high black hole kick model (magenta) the kicks are independent of the black hole mass and taken from a distribution with $\sigma = 265 \text{ km s}^{-1}$ (with an average kick of 420 km s^{-1}). Blue squares show available empirical estimates for Galactic black holes (see Table 2; if two values of a kick are measured for an object then an average is used in this plot). The red line representing our standard model shows kicks corresponding to single star solar metallicity evolution. Along this line we list initial (Zero Age Main Sequence) mass of the black hole progenitor in M_{\odot} (see the Appendix for a detailed explanation).

APPENDIX

BH MASS – KICK VELOCITY RELATION

In our standard model for natal kicks in core collapse SNe we employ a Maxwellian kick distribution with $\sigma = 265 \text{ km s}^{-1}$, based on observed velocities of single Galactic pulsars (Hobbs et al., 2005). The mass of the remnant object may generate a gravitational potential strong enough to prevent parts or all of the mass ejected during SN from reaching escape velocity. The matter falling back onto the remnant object will reduce the original (Maxwellian) kick velocity due to conservation of momentum. The more massive the final (pre-SN) core of the star, the more fallback it generates. In the asymmetric mass ejection kick mechanism (adopted here) this results in BH natal kicks being smaller than NS kicks. To account for this effect we use a simple linear relation for the reduction of natal kick magnitude by the amount of fallback during a SN:

$$V_k = V_{max}(1 - f_{fb}), \quad (\text{A1})$$

where V_k is the final magnitude of the natal kick, V_{max} is the velocity drawn from a Maxwellian kick distribution, and f_{fb} is the fallback factor. The values of f_{fb} range between 0–1, with 0 indicating no fallback/full kick and 1 representing total fallback/no kick (in this case a direct collapse).

Fig. 5 shows how BH natal kicks are related to the BH mass in a solar metallicity environment for our standard model (red line). In this model the minimum mass of a BH progenitor is $\sim 20 M_\odot$ at Zero Age Main Sequence (ZAMS), and they produce $\sim 7 M_\odot$ remnants. At the end of their lives, stars of this mass develop extended, high density layers of oxygen and silicon. When the nuclear evolution is completed, the infall of these layers stalls the SN explosion, resulting in a direct collapse to a BH. No matter is ejected and therefore no natal kicks are present. As we increase progenitor mass toward higher values, the final silicon and iron core masses and sizes increase. This results in the production of more massive BH remnants also through direct collapse. This trend continues until the progenitor mass reaches $\sim 30 M_\odot$ at ZAMS, corresponding to a BH mass of $\sim 8 M_\odot$.

Above $30 M_\odot$ this trend is temporarily disrupted. A star with such mass at ZAMS loses enough mass in stellar winds to strip itself of its hydrogen envelope and expose its helium core. Such objects, Wolf-Rayet (WR) stars, continue to lose mass at very high rates ($\sim 10^{-5} M_\odot \text{ yr}^{-1}$), and this extensive mass loss may lower the binding energy of the star, making it easier to explode.

Whereas mass-loss alters the star’s fate from the outside in, instabilities in shell burning at the end of nuclear evolution can alter the fate of the star from within the core. As we increase progenitor mass the core of the star grows in size and forces the shell burning layers toward the surface. At $\sim 30 M_\odot$ the core is large enough for the shell burning to occur at different temperatures. The extent and explosiveness of the shell burning is very sensitive to the exact conditions of the star such that shell burning can be very different for stars of nearly the same mass. The result is a dip in the final silicon and iron core masses. These smaller silicon and iron cores can lead to stronger explosion energies and lower remnant masses. Our standard model includes both of these effects (wind mass loss and shell burning instabilities). Their interplay results in the lowest amount of fallback during a SN explosion. As a consequence, the resulting remnant BH has the lowest mass ($\sim 5 M_\odot$) and the highest natal kick for a $\sim 30 M_\odot$ progenitor. However, note that both wind mass-loss and shell burning are open fields of research and their effects on remnant masses are likely to change quantitatively as we gain a more complete understanding of the underlying physics.

Increasing the progenitor mass beyond $30 M_\odot$ gradually increases the amount of fallback matter, which reduces the natal kicks and increases the final remnants mass. BH progenitors with masses over $\sim 90 M_\odot$ at ZAMS produce final silicon and iron cores massive enough for full fallback (direct collapse). As a result the kick velocities decrease to zero. A more detailed description of the supernova modeling is given in Fryer et al. (2012).